

**IMMOBILIZATION OF IRON ON CARBON NANOSPHERES BY TRIS-(1,10-PHENANTHROLINE) IRON (II) SULPHATE COMPLEX FOR SUPERCAPACITOR APPLICATIONS**

A thesis submitted for partial fulfillment  
for the requirement for the degree of

**MASTER OF SCIENCE  
IN  
CHEMISTRY**

submitted by

**Aashima**

(Roll No. 301702001)



**THAPAR INSTITUTE**  
OF ENGINEERING & TECHNOLOGY  
(Deemed to be University)

Under the Supervision of

**Dr. Manmohan Chhibber**  
Associate Professor, SCBC

**Dr. Loveleen Kaur Brar**  
Assistant Professor, SPMS

**School of Chemistry and Biochemistry**  
**Thapar Institute of Engineering and Technology**  
(Deemed to be University)  
**Patiala, India**

**July 2019**

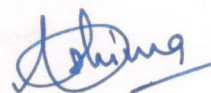
## ***Candidate's Declaration***

---

I hereby declare that the thesis entitled **IMMOBILIZATION OF IRON ON CARBON NANOSPHERES BY TRIS-(1,10-PHENANTHROLINE) IRON (II) SULPHATE COMPLEX FOR SUPERCAPACITOR APPLICATIONS** is an authentic record of my work carried out in partial fulfillment of the requirements for the award of the degree of Master of Science in Chemistry at Thapar Institute of Engineering and Technology, Patiala under supervision of Dr. Manmohan Chhibber Associate Professor, School of Chemistry and Biochemistry (SCBC) and Dr. Loveleen Kaur Brar, Assistant Professor, School of Physics and Material Sciences (SPMC), Thapar Institute of Engineering and Technology (TIET), Patiala during January 2017 to July 2019. No part of the matter embodied in this report has been submitted to any other university or institute for the award of any degree.

**Patiala**

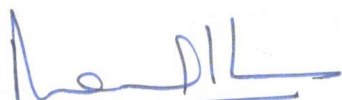
**Date: 15/07/19**



**Aashima**

**Roll no. 301702001**

It is certified that the above statement made by the student is correct to the best of my/our knowlowdge and belief.



**Dr. Manmohan Chhibber**

Associate Professor,

SCBC,

TIET, Patiala, Punjab-147004



**Dr. Loveleen Kaur Brar**

Assistant Professor,

SCBC,

TIET, Patiala, Punjab-147004

## **Acknowledgement**

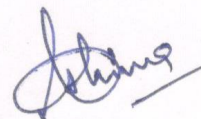
---

Foremost, I would like to express my deep sense of gratitude and obligations to my advisors, **Dr. Manmohan Chhibber**, Associate Professor, School of Chemistry and Biochemistry (SCBC) and **Dr. Loveleen Kaur Brar**, Assistant Professor, School of Physics and Material Sciences (SPMC), Thapar Institute of Engineering and Technology (TIET), Patiala, for their continuous support in my dissertation. I thank them for their patience, motivation and immense knowledge that carried me through the difficult times and for their insights and suggestions that helped me to shape my research skills. It is a matter of pride and pleasure that I had worked under their generous and able supervision.

I would like to thank all my honorable Professors of School of Chemistry and Biochemistry, TIET Patiala who have taught me. And I also thanks to **Dr. Amjad Ali**, Professor and Head of Department for providing his support and facilities to conduct this research.

A special thanks to **Ms Shiavli Gupta, Mr. Ashok Sharma, Ms. Raveena and Ms. Surbhi Sharma**, research scholars, for their help and valuable suggestions. I express my sincere thanks to my lab mates **Arashdeep and Anisha** for their valuable support. I am also thankful to all my friends **Hemant, Shagun, Kanika** for continuous moral and intellectual support.

Finally, I must express my very profound gratitude to my parents for providing me with unfailing support and continuous encouragement throughout my years of study. Last but not the least; I thank the Almighty for everything that I am blessed with.

  
**Aashima**

***DEDICATED***

***TO***

***MY BELOVED FAMILY***

**(Mr. Kapil Mahajan and Mrs. Anupama Mahajan)**

## ***CONTENTS***

<b>S.No</b>	<b>Chapters</b>	<b>Page No</b>
	<b>Abstract</b>	1
<b>I.</b>	<b>Chapter 1</b>	2
	Introduction	2
<b>II.</b>	<b>Chapter 2</b>	4
	Literature Review	4
<b>III.</b>	<b>Chapter 3</b>	
	Materials and Methods	10
<b>IV.</b>	<b>Chapter 4</b>	
	Result and Discussion	14
	Synthesis & Characterization	14
	Applications	20
<b>V.</b>	<b>Conclusion</b>	23
<b>VI.</b>	<b>Future Scope References</b>	23
<b>VII</b>	<b>References</b>	24

<b>LIST OF FIGURES</b>	<b>PAGE NO.</b>
Figure 1.1: Allotropes of carbon	2
Figure 1.2: SEM images of nanomaterials	2
Figure 1.3: TEM images of carbon nanospheres	3
Figure 2.1: Pd-coated nanospheres used for coupling reaction.	4
Figure 2.2 : Image of gas sensors and thin film coated on it.	4
Figure 2.3: Manufacturing process of elastic conductive composite.	5
Figure 2.4: Image showing fabrication process (Fe) N-P/CNS	5
Figure 2.5: Schematic elaboration for synthesis, drug delivery, modification on CNS.	6
Figure 2.6: Semihydrogenation of phenylacetylene.	7
Figure 2.7: Synthesis of 5-aminolevulinic acid from methyllevulinate.	7
Figure 2.8: Reduction of nitrophenol.	8
Figure 2.9: Schematic view showing the rechargeable Zn-air batteries (ZAB).	8
Figure 2.10: Schematic diagram CNS formation and its applications.	9
Figure 3.1: Characterisation of carbon nanospheres.	11
Figure 3.2: Attempted synthesis for aniline.	13
Scheme 4.1: Synthesis of 1,10-phenanthroline formation of red coloured powder.	15
Figure 4.1: Synthesised tris- (1,10-phenanthroline)iron.	16
Figure 4.2: Supernatant showing decreasing concentration tris-(1,10-phenanthroline) iron (III) complex with increasing CNS amount.	17
Figure 4.3: UV-Visible Spectra of supernatant.	18
Figure 4.4: FTIR spectra showing difference in absorbance in bare-CNS and Fe immobilised CNS.	19
Figure 4.5 (a): SEM image of Fe <sub>2</sub> CNS (2:1).	19
Figure 4.5 (b): SEM image of Fe <sub>10</sub> CNS (10:1).	20
Figure 4.6: EDS Data.	21
Figure 4.7: BET Data.	21
Figure 4.8: Showing degradation of Methylene Blue UV light and absorption in dark.	22

Figure4.9: Graph plotted between potential and current density showing CV when Fe10CNS is used as working electrode.	22
Figure 4.10(a): Graph plotted between potential and current density showing comparison of voltammetry cycle between Bare-CNS, Fe2 CNS and Fe10CNS.	23
Figure4.10 (b): $C_{dl}$ fits for all the samples.	23

<b>LIST OF TABLES</b>	<b>PAGE NO.</b>
Table 3.1: BET results of bare- CNS.	11
Table 3.2: Showing the synthesis of Fe immobilized CNS.	12
Table 3.3: Trail reaction for synthesis of aniline using different solvent, reagents and at varying reaction conditions.	13
Table 4.1: Functional groups and there corresponding peaks present in FTIR spectra.	16
Table 4.2: FTIR values of CNS.	18
Table4.3: Elements present in sample.	20
Table 4.4: Calculated $C_{dl}$ value for samples.	24

## ABSTRACT

---

Uniform and mesoporous carbon nanospheres (CNS) have great applications in many areas of science like supercapacitor, catalyst, batteries and many more. This work describes immobilization of iron on surface of CNS by sonication method. Preformed CNS of average diameter of 470nm, prepared by hydrothermal method was used. A well-known organometalic compound, tris-(1,10-phenanthroline)-iron (II) sulphate was used for the immobilization purpose. All the materials were characterised using UV-Visible Spectroscopy, FTIR, SEM and BET surface area analyzer as applicable. Three different samples of CNS having varying percentage of iron were synthesized. The samples were further used in decolorisation of methylene blue dye by absorption in dark and degradation in UV light. The degradation decreased from 80% by bare CNS to 64% by Fe immobilized CNS but absorption of dye increased from 27% to 37.5% in dark. The Fe immobilized CNS were also demonstrated for super capacitor applications as electrode and  $C_{dl}$  value was best for CNS partially immobilized with Fe.

## CHAPTER 1

### INTRODUCTION

Carbon is one of the most versatile elements of periodic table. Its hybridization state and atomic arrangement can lead to wide range of carbonaceous structures having different properties. The science of carbon is in demand in the fields of nanoscience, material science, engineering and technology, due to its different allotropic forms<sup>[1]</sup>. Graphite as named by Abraham Gottlob Werner in 1789 comprises of infinite layers of  $sp^2$ - hybridized carbon atoms forming a flat network (**Figure 1.1**). The material is an excellent electrical conductor and used as electrode in electrical arc lamps. Diamond, on other hand, is the hardest allotropic form of carbon and most stable thermodynamically above 60K bar<sup>[2]</sup>.

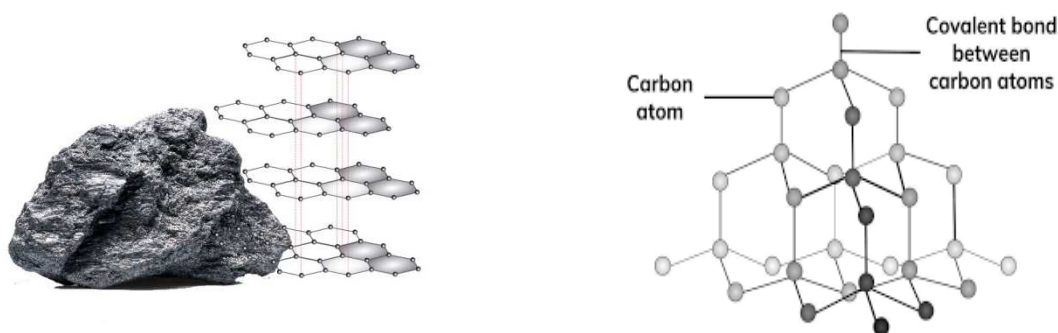


**Figure 1.1:** Allotropes of carbon (a) Graphene showing infinite layers (b) Diamond showing bonding of carbon atom.

Interestingly, conventional occurring allotropic form of carbon namely graphite and diamond now has other additions as well. In 1996, Kroto, Curl and Smalley were awarded nobel prize for chemistry for the discovery of third allotope form of carbon named fullerene (**Figure 1.2 a**). This hydrophobic highly conjugated electron deficient substance was later made into water soluble material that resulted into diverse molecules that had potential applications like artificial photosynthesis, surface coating, drug and gene delivery materials besides in cosmetic<sup>[3]</sup>. Before this, Iijima, in 1991, reported synthesis of carbon nanotubes that had layers of concentric cylinders ranging from 0.4– 500 nm<sup>[4]</sup> (**Figure 1.2 b**). Unique physiochemical properties of the nanotubes made it an efficient material for adsorption, catalysis, H<sub>2</sub> storage and many more electronic applications<sup>[5]</sup>. Recently, Geim *et. al.* reported  $sp^2$  carbon lattice of one atom thickness having honeycomb structure called graphene<sup>[6]</sup> (**Figure 1.2 c**). The material was a marvellous discovery because of its very basic nature<sup>[7]</sup>. For example, sheets of graphene could be stacked on top of each other to form graphite and if

rolled up in one up in one direction around a centre form nanotubes of desired shapes. Similarly, if the same material rolled up around one point in all the three dimensions could give fullerenes [7]. Further work led to the discovery of flakes and nanoribbons [8]. All the above materials due to their mechanical, electrical and thermal properties have applications in sensing , solar cells, circuits, electrode materials, light-emitting diodes and batteries [9-13].

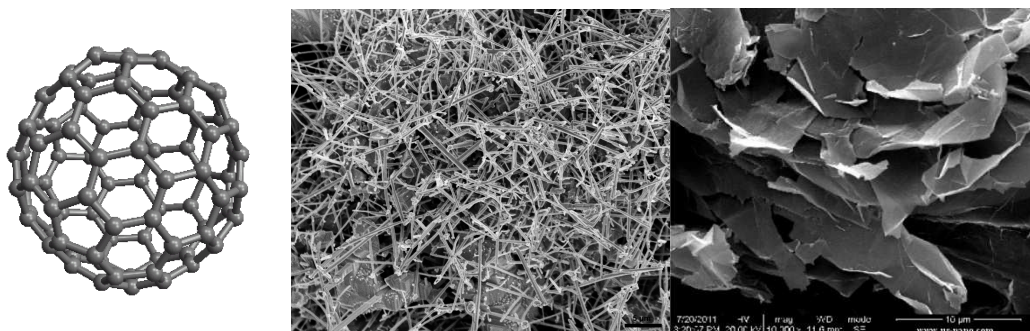


**Figure 1.2:** Advancement in carbon nanomaterials (a) C<sub>60</sub> structure of fullerenes (b) SEM image of carbon nanotubes (c) SEM image of graphene sheets.

Besides the carbon materials described above, carbon nanospheres (CNS) are recent spherical concentric graphitic materials formed by pairing of carbon rings having pentagonal and heptagonal shapes [5]. Depending upon the conditions in which they are formed their size ranges from 50 nm and 1 $\mu$ m as shown by SEM and TEM images in **Figure 1.3**. [14]. Dangling hydroxyl groups on the surface and their porous nature makes them another good catalytic material for adsorption studies. Of all the nanomaterials discussed above CNS are known to have enormous applications in optoelectronics, medicines, gas storage and sensors, heterogeneous catalysts and for encapsulating electrodes [14].

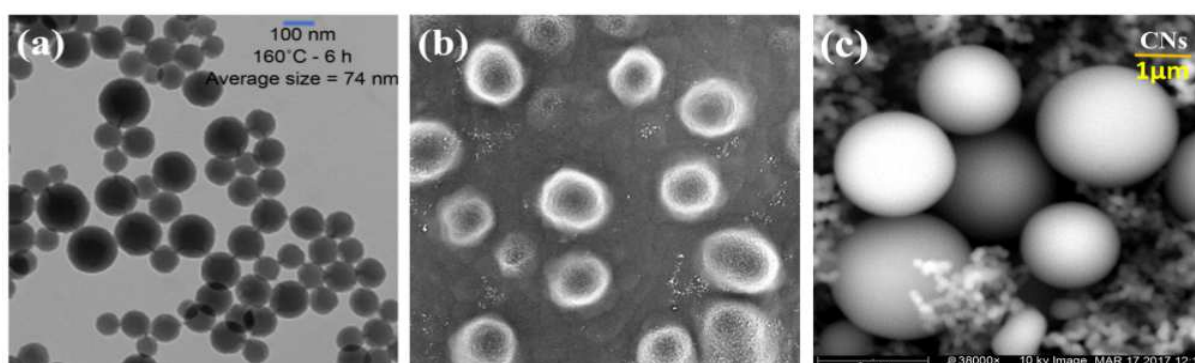


**Figure 1.3:** Spherical shape of CNS (a) TEM image of CNS synthesised for 6hrs (b) Spheres are porous (c) SEM images of CNS at 1 $\mu$ m.

The work presented in this thesis deals with modifying the surface of CNS with complex of organometallic iron complexes and their application as super capacitors.

REVIEW OF LITERATURE

In the early 2000 scientists made use of nanospheres having functional groups and metals, which were made by different types of polymerisation techniques and further had great utility in different fields as described in some of the literature references.

In the year 2000 Pathak and his co-workers made Pd coated nanospheres which were characterized by TEM and coupled plasma mass spectrometry (**Figure 2.1**). The material served as a good catalyst for coupling reaction like Heck, Stille and Suzuki <sup>[15]</sup>.

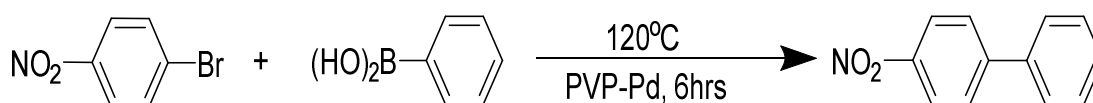


**Figure 2.1:** Pd-coated nanospheres used for coupling reaction.

Work has been reported in using Pt as a catalyst for production of hydrogen gas from methane and also directly from methonal for use in fuel cell. However, Pt is an expense metal and therefore Liang *et-al* in 2004 made use of Pt- hollow nanospheres to make it economical and cost effective. The advantage was that Pt catalyst with high surface area gave good catalytic performance and its utilization <sup>[16]</sup>.

In 2005 porous gold nanospheres were reported for their use in cell imaging techniques by use of fluorescent dye, propidium iodide (PI) that enhanced the surface area for binding. Besdies this, nanospheres are also used in various other applications like catalysis, drug delivery, enzymes immobilization and many more <sup>[17]</sup>.

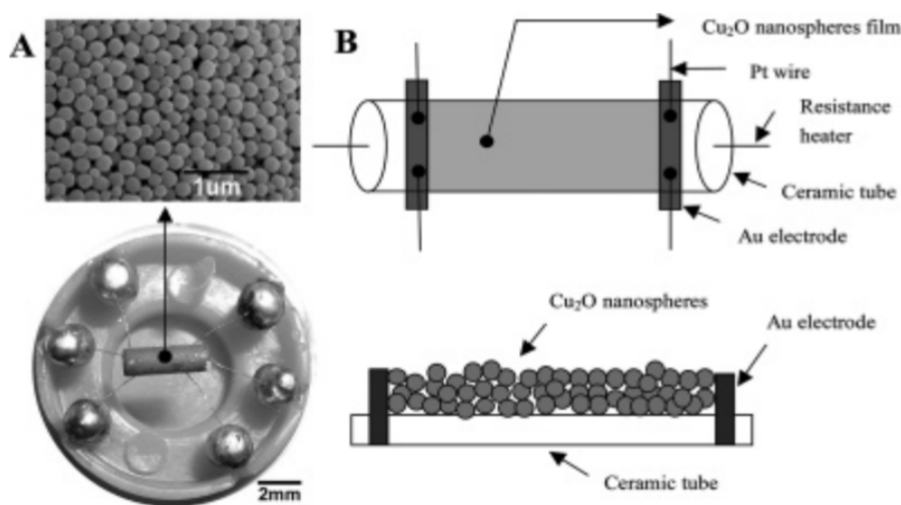


**Figure 2.2:** Image of gas sensors and thin film coated on it.

Zhang and his co-workers in 2006 reported use of monodisperse Cu<sub>2</sub>O and CuO nanospheres for gas sensing applications (**Figure 2.2**)<sup>[18]</sup>.

The advent of CNS for use in above mentioned applications as described in chapter-1 above, scientists discovered different processes for the formation of CNS. Also, carbon being the cost effective material is known to exist in versatile forms such as powder, fibre and composite<sup>[19]</sup> and can be used for functionalization, immobilisation and absorption applications.

**Arc discharge process** uses high temperature generated by discharge arc so that carbon atom ejected from the anode and is accumulated as solid carbon nanospheres at the cathode<sup>[20]</sup>.

In **chemical vapour deposition (CVD)** volatile carbon precursor, when exposed to certain conditions change to carbon nanospheres. Depending upon conditions used CVD can be achieved in different ways like direct liquid injection, atomic-layer of CVD, hot filament process and so on<sup>[21]</sup>.

In **laser vaporisation and plasma progression** the carbon source in the presence of metal catalyst is laser vaporized using a pulse of light into atoms and molecules within hot laser plasma. CNS in this process are generated according to the requirement as per choice of the electrode.

**Hydrothermal carbonisation** produces hollow CNS with diameters of few microns with reactive surface and controllable void size. Glucose is used as a starting material in presence of anionic surfactants in hydrothermal process that is normally done at around 180°C. A large number of carbon sources such as sucrose, cellulose, xylose, maltose, amylopectin, and starch have been reported for the purpose<sup>[21]</sup>.

**Reduction method** involves use of autoclave to produce CNS. Here, different sizes can be generated depending upon the concentration of carbon precursor. Reactant can be any carbon material that is subjected to high pressure in an auto-clave under variable thermal conditions.

**Shock compression method** uses carbon source at high temperature, by direct pyrolysis to convert fullerenes to carbon nanospheres<sup>[22]</sup>.

Carbon nanospheres are in great demand today due to their diverse applications in various fields. Some of different applications of the material have been described in following paragraphs.

A highly stretchable conductive polymer composite of carbon nanotubes and nanospheres was prepared by Shang *et. al.* in 2010 (**Figure 2.3**). The material was used as chemically stable dopants in high utility polyurethane matrix in uniformly a dispersed form<sup>[23]</sup>. Also, these nanocomposite polymers possessed both high conductivity and high elasticity which lead to great application in high performance electronic circuit.

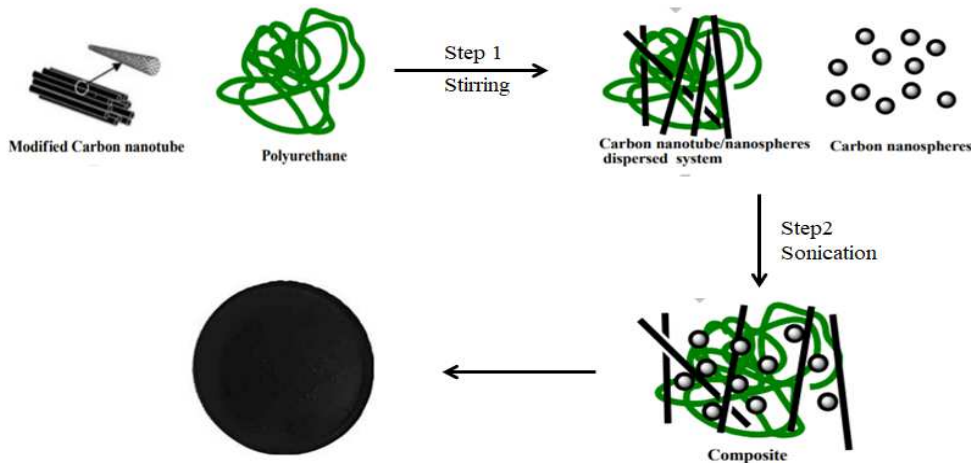


**Figure2.3:** Manufacturing process of elastic conductive composite.

Further research in the field displayed use of hollow carbon nanospheres for the superior capability sodium based batteries as an alternative for lithium ion batteries due to the low cost and high natural abundance of the metal<sup>[24]</sup>. Sodium ion uptake in the disordered form of carbon showed a charge/discharge curve similar to that of lithium for a convenient use<sup>[25]</sup>.

CNS were also used as adsorbent for removal of arsenate and selenate in de-ionization of canals and well waters even at  $\text{pH} > 8$ . It was reasoned that the presence of basic surface functional groups, high surface-to-volume ratio and pores formed during manufacturing were facilitating the adsorption phenomena<sup>[26]</sup>.

Synthesized carbon nanospheres were developed into inkjet-printed resistive layers and sensors by Viét-*al.* in 2015. Impressingly, CNS appear to be a well-adapted material for the development of accurate sensors<sup>[27]</sup>.

There are also reports of oxygen reduction reaction by nitrogen, phosphorus and iron-doped carbon nanospheres with high surface area. The catalyst displayed excellent electrocatalytic performance with iron and phosphorus salts at its surface (**Figure 2.4**). It was rationalized that the increase in catalytic effect was due to **a)** synergistic effect which provides more sites for the reduction reaction, **b)** presence of Fe on the surface and **c)** high surface area<sup>[28]</sup>.

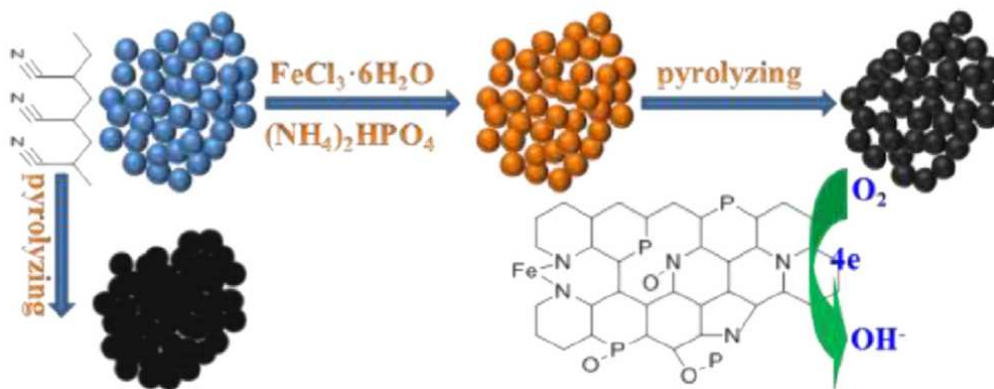


**Figure 2.4:** Image showing fabrication process (Fe) N-P/CNS.

In 2016, Wang and co-workers discovered that hydrophilic mesoporous carbon nanospheres have high drug-loading efficiency for a medicine used in cancer therapy, doxorubicin (**Figure 2.5**). The results showed good efficiency of CNS to penetrate the membrane tumour cells, release drug and inhibit the growth of tumour cells [29].

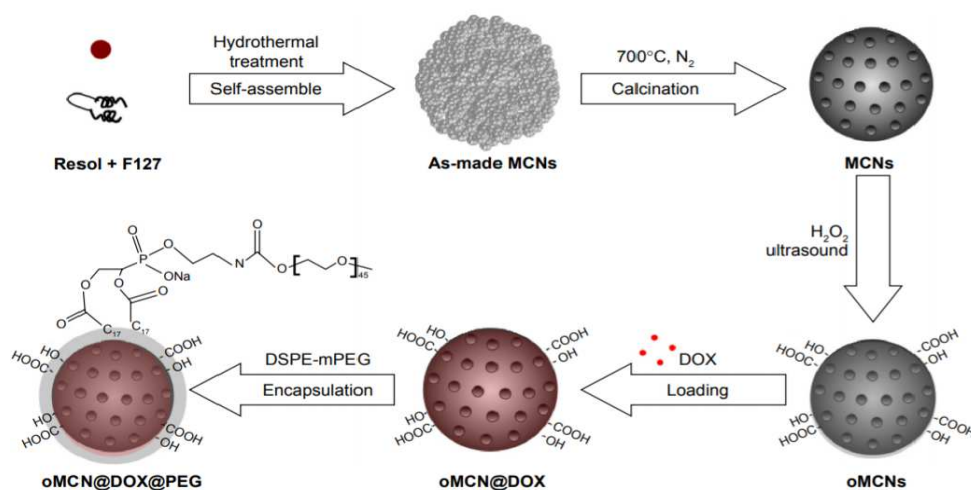


**Figure 2.5:** Schematic elaboration for synthesis, drug delivery, modification on CNS

Zhang *et. al.* carried out semihydrogenation of phenylacetylene in different solvents using CNS immobilized with Pd nanoparticles introduced with both Fe and N as a catalysts as shown in **Figure 2.6** [30].

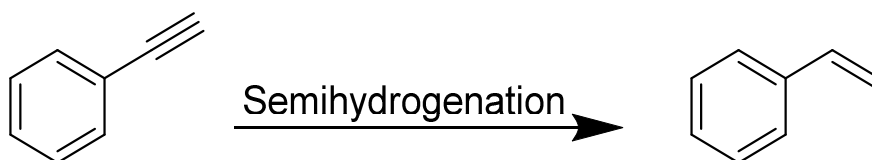


**Figure 2.6:** Semihydrogenation of phenyl acetylene.

Gupta and co- worker used CNS supported with Ru catalyst for synthesis of renewable herbicide and chemicals as shown in **Figure 2.7** <sup>[31]</sup>.

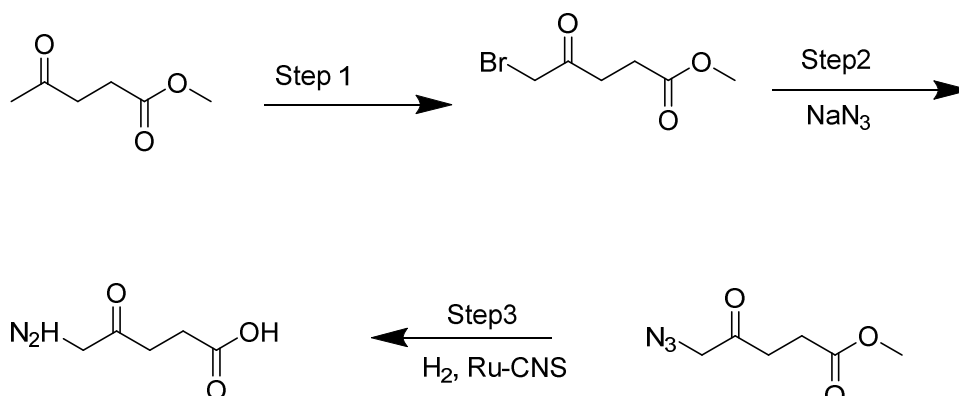


**Figure 2.7:** Synthesis of 5-aminolevulinic acid from methyllevulinate.

A new material composed of amorphous PdP nanoparticles supported on CNS was used for the reduction of 4-nitrophenol. The catalysis was carried out with 95% efficiency and reusability upto seven cycles (**Figure 2.8**) <sup>[32]</sup>.

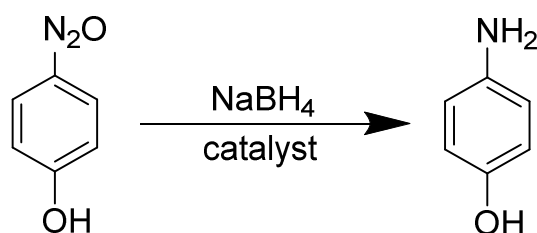


**Figure 2.8:** Reduction of nitrophenol.

Taoa *et. al.* used N, P, S tri-doped hollow carbon nanosphere as a high-efficient bifunctional oxygen electrocatalyst for rechargeable Zn-air batteries (**Figure 2.9**) <sup>[33]</sup>. NPSCSs composite were synthesised using template-induced polymer-derived strategy

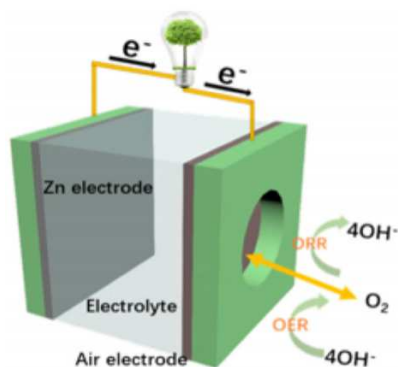


**Figure 2.9:** Schematic view showing the rechargeable Zn-air batteries (ZAB).

Wang and his co-workers produced bifunctional catalysts and demonstrated the use of carbon nanospheres as air electrode lithium-air batteries. *In situ* growth of  $\text{Co}_3\text{O}_4$  on nitrogen-doped hollow carbonnanospheres gave the desired catalyst that could work upto 27 charge/discharge cycles. However it stopped working after that due to the accumulation of discharge products on the electrode <sup>[34]</sup>.

A multi futional - nanoporous carbon nanospheres were formed by conversion of plant polyphenol like tannic acid. Zinc content of CNS played an important role in its porosity. The material was further used for sensing nucleic acid variants with high selectivity and low detection limit and as an electrode material (**Figure 2.10**). The super capacitor material had good capacitor retention capabilty and cyclic stability <sup>[35]</sup>.



**Figure 2.10:** Schematic diagram CNS formation and its applications.

Song and his co-workers used carbon nanospheres which adsorbed Ag from drinking water production and this catalyst is cost effective. Surface of CNS was enriched with  $-\text{OH}$  and  $-\text{COO}^-$  functional groups by using  $\text{NaOH}$  for activation. The adsorbed Ag can be recovered by treating with dilute acid solution and CNS is again activated by treating with  $\text{NaOH}$  <sup>[36]</sup>.

Work describes in next sections demonstrates immobilization of iron, in different ratios, on the surface of pre-prepared CNS by sonication method using a well-known organometalic compound, tris-(1,10-phenanthroline)-iron (II) sulphate followed by its application for dye degradation and for super capacitor as electrode material.

## CHAPTER 3

---

### MATERIALS AND METHODS

**Chemical:** All the chemicals used were purchased from different sources and were of 98% purity or higher. 1,10-Phenanthroline, FeSO<sub>4</sub> and ethanol were purchased from Sigma Aldrich, Avra Chemicals, and Spectrochem Limited respectively. Double distilled water was used for all the dilutions and washings. It was obtained from a distillation glass apparatus installed in the School of Chemistry and Biochemistry.

**Instrumentation:** Characterization of the synthesised product was done using different instruments. Scanning electron microscope, SEM (JEOL, JSM, 6510LV, SAI Labs, Patiala, India), FTIR (SAIF, Punjab University, Chandigarh, India) with KBr matrix, UV-Vis spectrophotometer (Hitachi, U-3900H, SPMS, TIET, Patiala, India) and BET surface area analyzer (SCBC, TIET, Patiala, India) was used for different analysis of the CNS or the supernatants to determine size, morphology, topography, pore volume and functional group presence etc. The centrifuge machine (Thermofisher Scientific) and the sonicator (Branson 3510) were used for collection & dispersion of various CNS samples.

**Synthesis of Carbon nanospheres:** Uniform, monodispersed CNS synthesized from sucrose through hydrothermal process were obtained from LKB's lab, School of Physics and Material Science, Thapar Institute of Engineering and Technology, Patiala. SEM, BET isotherm and porosity of the material were already known as shown in **Figure 3.1** below.

**Synthesis of tris-(1,10-phenanthroline) iron (II) sulphate:** 1,10-Phenanthroline (400mg, 2.2mmol) was taken in a 100 ml round bottom flask and dissolved in ethanol (5mL) using a magnetic stirrer. After 10 minutes iron (III) sulphate (606 mg, 3.9 mmol) was added drop wise to get a red coloured solution that was precipitated using dropwise addition of cold ethanol (10mL). Filtration of the red coloured precipitates using a Buckner funnel and vacuum gave a solid powder that was dried in a hot air oven at 70<sup>0</sup>C for 16 hours. The red coloured powder was characterized using FT-IR and UV-Visible spectrophotometer (**Figure 4.1 b and C**).

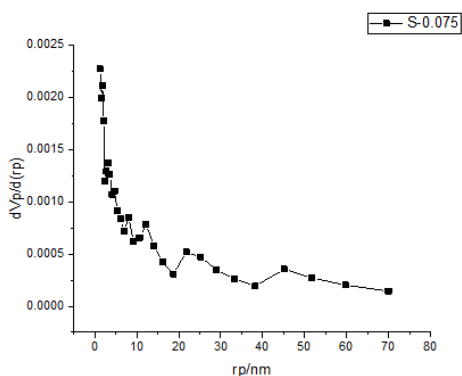
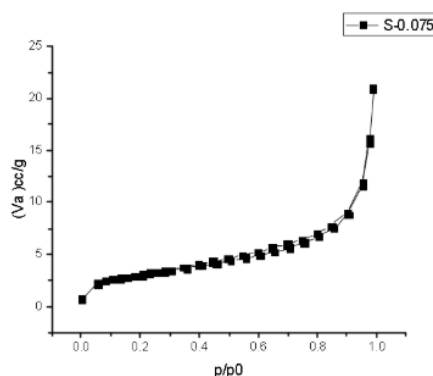
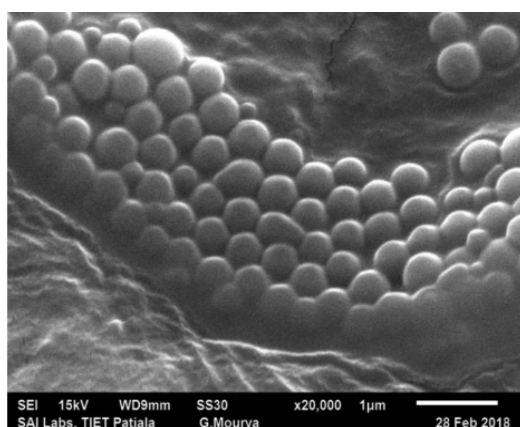
**Synthesis of iron immobilized CNS: Immobilization of Fe on carbon nanospheres:** Two stock solutions, one of CNS and the other of the above synthesized tris-(1,10-phenanthroline) iron (II) sulphate, were prepared.

For CNS stock, distilled water (1ml) was added to 20mg of CNS and sonicated for half an hour to make them homogeneously dispersed.

For Fe-1,10-phenanthraline complex, stock (178mg) of the complex was dissolved in 30mL of distilled water to get a concentration of  $10^{-2}$ M. Further dilution of the stock gave a concentration ( $10^{-4}$ M ) of Fe-1,10-phenanthraline that was used for the immobilization. Three different reaction mixtures of samples Fe2CNS, Fe5CNS, and Fe10CNS were prepared as shown in **Table 3.2** and sonicated for 1 hour to get the iron immobilized on the surface of CNS.

After cooling to room temperature the mixture was centrifuged to settle the product and supernatant removed using pipette for UV analysis. Immobilized CNS were dried overnight in hot air oven at  $70^{\circ}\text{C}$  and characterized using FTIR, SEM-EDX and BET surface area analysis. Supernatant was also analysed for the presence of complex or other products using UV-Visible spectrophotometer.

**Photocatalytic activity of CNS:** Nano material can act as catalyst and speed up the photo reaction in presence of light (Ultraviolet, sunlight) is an important property of photo catalysis. Photo catalytic activity depends on ability of a catalyst to create electron-hole pairs. CNS was used to degrade methylene blue as a contaminant under UV- Visible light irradiation.



Mean pore diameter	11.91 nm
Total pore diameter	0.03 cm <sup>3</sup> /g
BET surface area	10.9m <sup>2</sup> /g

**Figure 3.1:** Characterisation of carbon nanospheres **a)** SEM image<sup>37</sup> **b)** N<sub>2</sub> adsorption and desorption isotherms of bare-CNS **c)** pore size distribution of bare-CNS.

**Table 3.1:** BET results of bare- CNS.

S.No.	SAMPLE ID	STOCK CNS	STOCK OF Fe-1,10-phenanthraline complex (10 <sup>-4</sup> M)	DISTILLED WATER
1.	Fe2CNS	100µL (2mg)	10µL	890 µL
2.	Fe5CNS	250 µL (5mg)	10µL	730 µL
3.	Fe10CNS	500 µL (10mg)	10µL	490 µL

The experiment was performed in photo reactor which consisted of a cylindrical glass vessel in presence of UV light. 1 mg of CNS as a catalyst was dissolved in 50 mL of methylene blue (1mg in 1L of water) stirred for 2 hours. A second set of experiment was also performed in dark by simple stirring at room temperature. After completion of time CNS were separated from dye solution using centrifuge machine. The absorption spectra of methylene blue dye was observed at 664 nm by UV- visible spectrophotometer.

**Electrochemical Capacitance measurements:** The electro catalytic capacitance performance of the Bare-CNS, Fe2CNS, Fe10CNS in basic medium was done by using standard three electrode setup in a Bio-Logic EC Lab SP300. The reference electrode use was saturated calomel electrode with the platinum as counter electrode and a glassy carbon electrode loaded with sample as the working electrode. These electrodes used for electrochemical studies were immersed in 0.5 M KOH solutions. Prior to the actual measurement, for the removal of contamination on the surface, the pre-treatment of the working electrode/sample was done by cycling the potential between -2.5 V to 2.5 V (sweep rate of 20 mV/s for 30 cycles) which led to catalyst activation and electrochemical current stabilization. For the determination of the electrochemical capacitance, the recording of the cyclic-voltammety (CV) was done in the range of -2.5V to 2.5 V at different scan rates (5-200 mV/s). C<sub>dl</sub> Calculations were done for current densities at 0.0 V.

**Electrode fabrication:** For the preparation of the working electrode, considered sample (~1.0 mg) was dispersed in ethanol (250 µL) and Nafion®117 (Sigma Aldrich; 40.0 µL) through ultra sonication (30 min). After that 20 µL dispersed solution was drop-casted on the

cross-section of GCE ( $A = 0.07065 \text{ cm}^2$ ;  $\phi = 3 \text{ mm}$ ) and dried overnight at room-temperature providing the catalyst loading  $\sim 0.976 \text{ mg/cm}^2$ .

**Attempted synthesis of aniline from nitrobenzene (Figure 3.2):** CNS were used as catalyst for reduction of nitrobenzene. Reaction was carried out in an eppendorf, round bottom flask, pressure tubes using different solvents and reagents for reduction. Reaction was performed using CNS, Fe10CNS (2mg) which was first sonicated so that CNS gets disperse in solution. **Table 3.3** shows use of different reducing agents and conditions applied to for the completion of attempted reaction reaction.

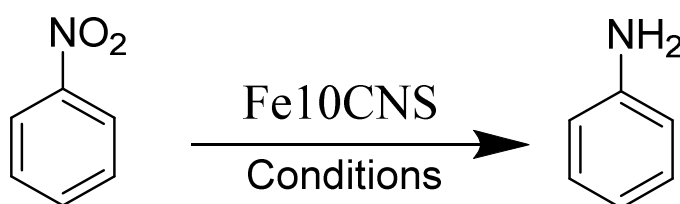


**Figure 3.2:** Attempted synthesis for Aniline.

**Table 3.3:** Trail reaction for synthesis of aniline using different solvent, reagents and at varying reaction conditions.

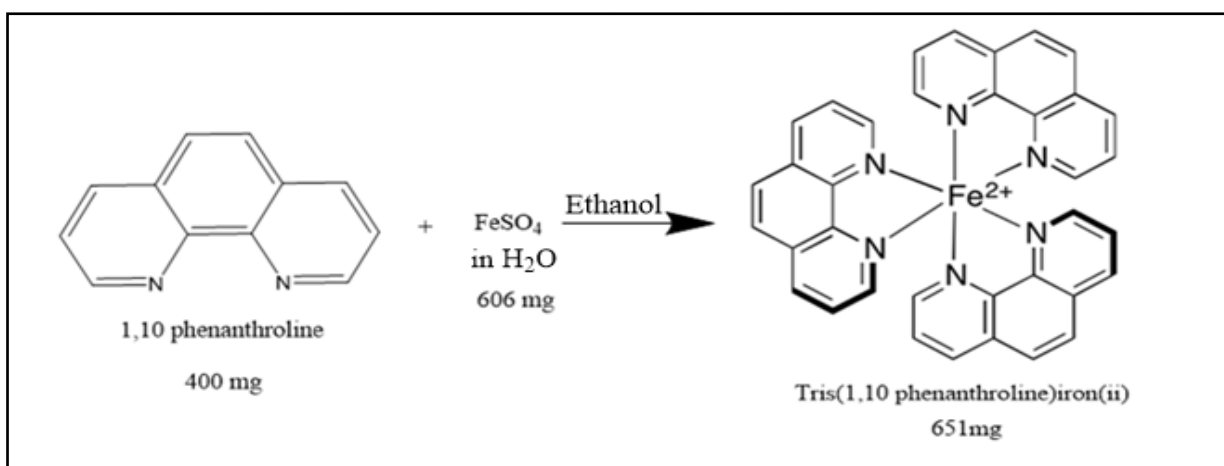
S.NO.	REDUCING AGENT	SOLVENT	CONDITIONS	TIME	REMARKS
1.	NaBH <sub>4</sub> (2mg, 0.05mmol)	Water	Thermal	12hrs	HCl + Zn(NO <sub>3</sub> ) <sub>2</sub>
2.	NaBH <sub>4</sub> (9mg, 0.23 mmol)	Ethanol	Sonication	2hrs	Zn(NO <sub>3</sub> ) <sub>2</sub>
3.	Hydrazine (10μL, 0.5 mmol)	Water/ DMSO	Sonication	7hrs	-
4.	Hydrazine hydrate (10μL, 0.5 mmol)	Acetonitrile/ THF	Thermal	18hrs	-
5.	Hydrazine hydrate (10μL, 0.5mmol)	Acetonitrile	Sunlight + Stirring	8hrs	-
6.	Hydrazine hydrate (10μL, 0.5nmol)	Acetonitrile	UV- photo reactor	12hrs	-
7.	Hydrazine hydrate (10μL, 0.5mmol)	Acetonitrile	Thermal	18hrs	+ NiCl +1,10 - phenanthroline

## CHAPTER-4

### RESULTS AND DISCUSSION

This section describes synthesis and characterization of iron carrier complex of 1,10-phenanthroline with Fe(II), followed by immobilization of iron on CNS. Later part of this chapter describes the application of synthesized material for methylene blue dye degradation and this use as a supercapacitor.

**4.1 Synthesis of tris-(1,10-phenanthroline) iron (II) sulphate complex:** The complex was synthesised by known method <sup>[38]</sup>. (Scheme-4.1) Ligand 1,10-phenanthroline was dissolved in ethanol and an equivalent amount of iron sulphate dissolved in water added dropwise. Appearance of tris- (1,10-phenanthroline) iron (II) complex confirmed its formation. The complex was precipitated by addition of excess of ethanol to be solution, followed by filtration using vacuum and drying in oven at 70°C for 18 hours (Figure 4.1 a).



**Characterization of tris- (1,10-phenanthroline) iron (II) complex:** was done by FTIR and UV-Visible Spectroscopy. Appearance of a distinguished band at 500 nm (Figure 4.1 b) in UV – Visible spectroscopy due to charge transfer complex confirmed the formation of tris-(1,10-phenanthroline) iron (II) complex. Result of IR spectra also corroborated the formation of product. The signals at 1200-1025 cm<sup>-1</sup>, 1480-1660 cm<sup>-1</sup>, 620.7 cm<sup>-1</sup> for C-N, C=N and SO<sub>3</sub><sup>2-</sup> respectively indicated the presence of ligand and counter ion for Fe(II).

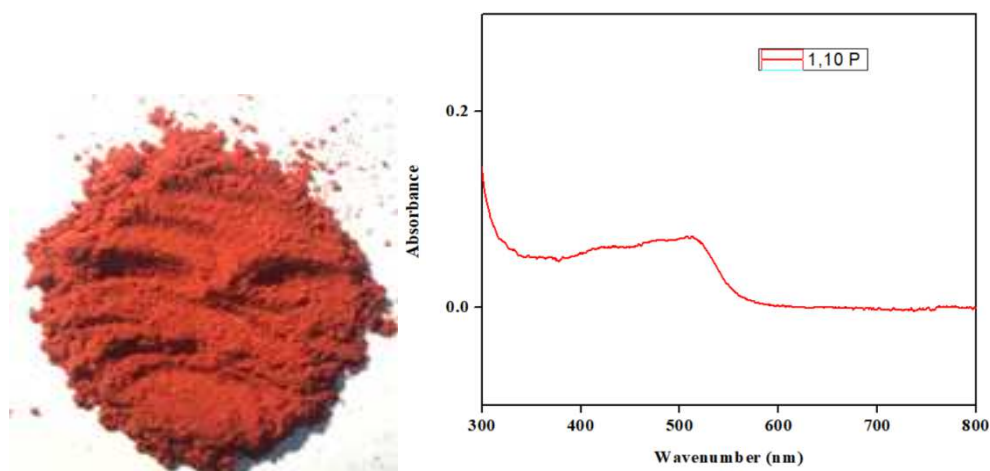
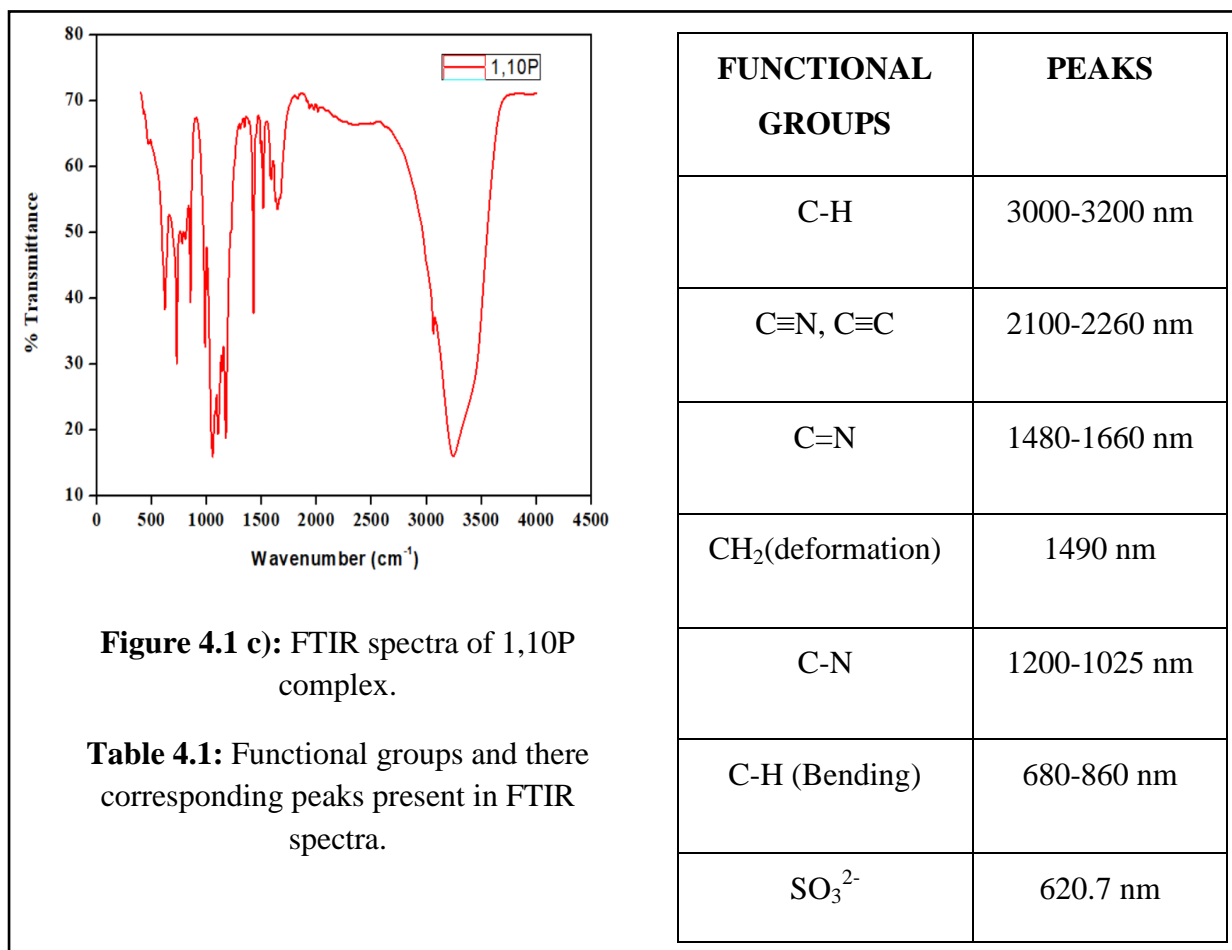


**Figure 4.1:** Synthesised tris-(1,10- phenanthroline) iron(ii) complex **a)** Red colour powder **b)** UV spectra showing peak of complex at 500 nm.



**4.2 Synthesis of Fe immobilized CNS:** Kumar *et-al* have reported immobilization of Iron – bipyridyl complex on graphene oxide surface and its use for photocatalytic reduction of

nitrobenzene. A similar procedure for the immobilization of iron on CNS was followed with slight modification in this case.

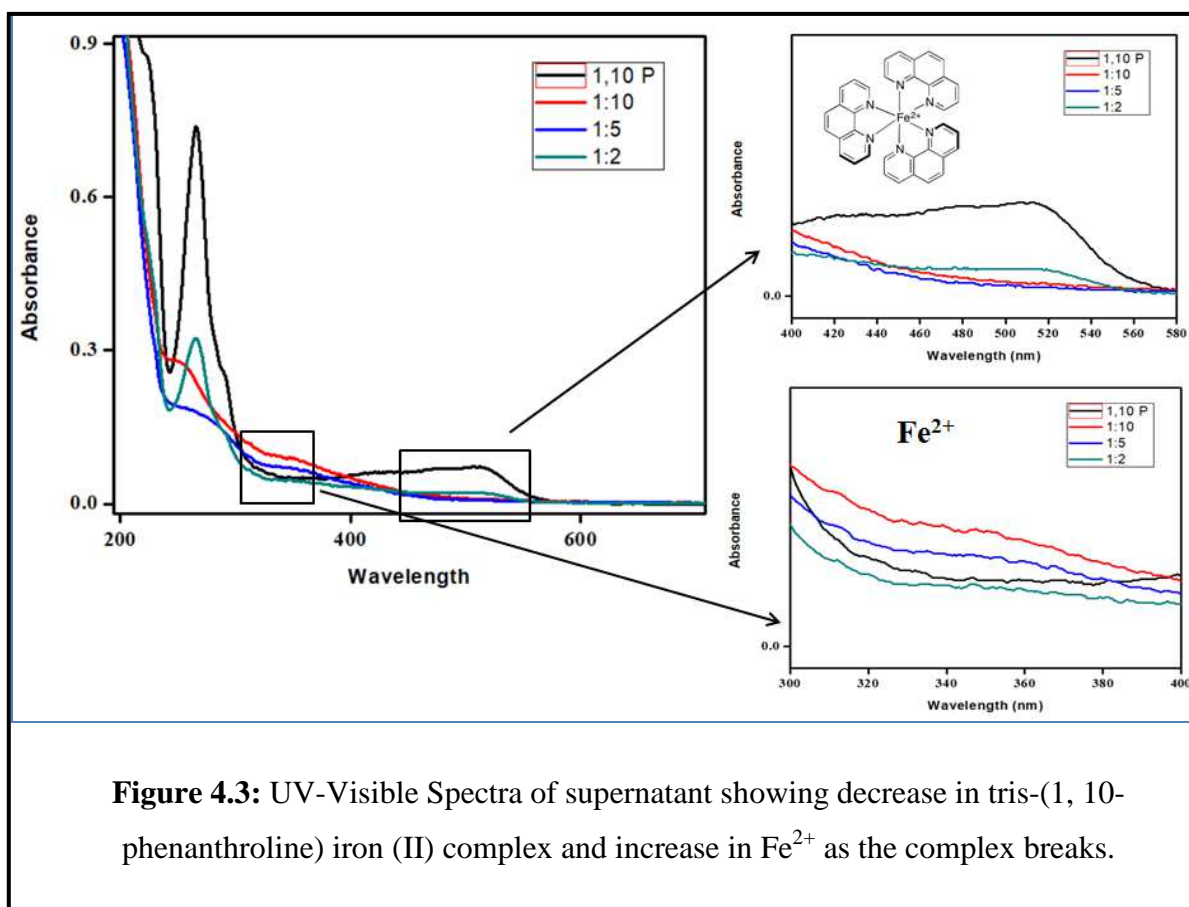
For immobilization of Fe the 1 $\mu$ M solution/dispersion of Fe-1,10-phenanthroline in water is prepared by sonication for 1 hour. Three different samples namely Fe2CNS, Fe5CNS, Fe10CNS were prepared by addition of 2mg, 5mg, 10mg of CNS in 1mL of Fe-1,10-phenanthroline dispersion respectively followed by 1 hour sonication. The samples after the immobilization were centrifuged to remove the supernatant and leaving behind a black solid mass consisting of CNSs at base. The solid mass remaining was dried overnight in hot air oven and the black mass obtained was characterized and used further.

The supernatant in each case (as shown in **Figure 4.2**) showed change in colour intensity due to different quantities of CNSs taken initially. Fe10CNS sample supernatant (**Figure 4.2 (c)**) was completely transparent as compared to Fe2CNS and Fe5CNS samples indicating the absence of any Fe-1,10-phenanthroline complex in supernatant. It can be inferred that higher available concentrations of CNSs the Fe-1,10-phenanthroline complex available in the dispersion completely breakdown since more area is available for Fe immobilization. While for lower concentration of CNSs even after complete immobilization of iron on the added CNS were left with residual quantity of the complex. This conjecture has been confirmed by the UV-Visible spectrum (Fig 4.3). Adsorption at 500nm shows decrease in concentration of 1,10-phenanthroline complex as the amount of CNS increase. The adsorption band at 340 nm for free 1,10-phenanthroline shows maximum adsorption for Fe10CNS indicating that Fe-1,10-phenanthroline complex has been broken down. Fe<sup>2+</sup> ions peak was maximum in case of Fe10CNS and least in Fe2CNS shows that complex breaks as we increase the CNS concentration.



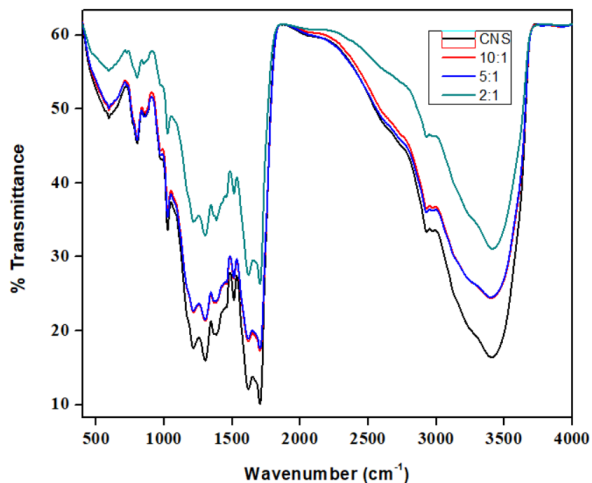
This is also supplemented by peak at 500nm for Fe-1,10-phenanthroline complex. **Figure 4.3 (c)** shows maximum intensity for native Fe-1,10-P complex followed by for the supernatant

of Fe<sub>2</sub>CNS, indicating its presence in 2mg sample. For Fe<sub>5</sub>CNS and Fe<sub>10</sub>CNS, 5mg and 10mg CNS samples this peak touches baselines indicating absence of any Fe-1,10-phenanthraline complex.



**FTIR Analysis:** Figure 4.4 shows comparable IR spectrum for iron immobilized carbon nanospheres. It can be seen that native CNS without any immobilization of iron show minimum transmittance while Fe<sub>2</sub>CNS having minimum amount of CNS (2mg) and thus maximum immobilization of iron display maximum transmittance.

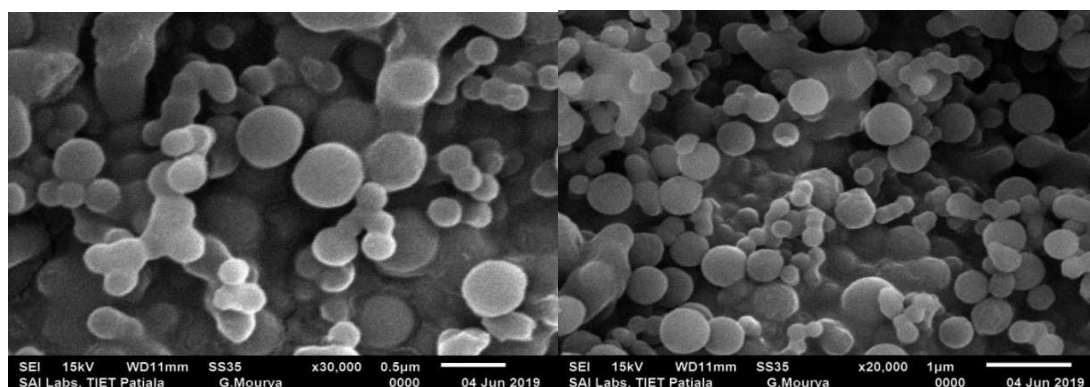
It can be inferred that adsorption of IR radiation which is reciprocal of transmittance, is maximum for bare organic CNS and is minimum for Fe<sub>2</sub>CNS because of its surface completely covered by the metal species. The adsorption for Fe<sub>5</sub>CNS and Fe<sub>10</sub>CNS samples lied in between these two extremes indicating that surface of these CNS samples was partially covered with iron. **Table 4.1** shows characteristic functional group present on the surface of CNS with their literature values.



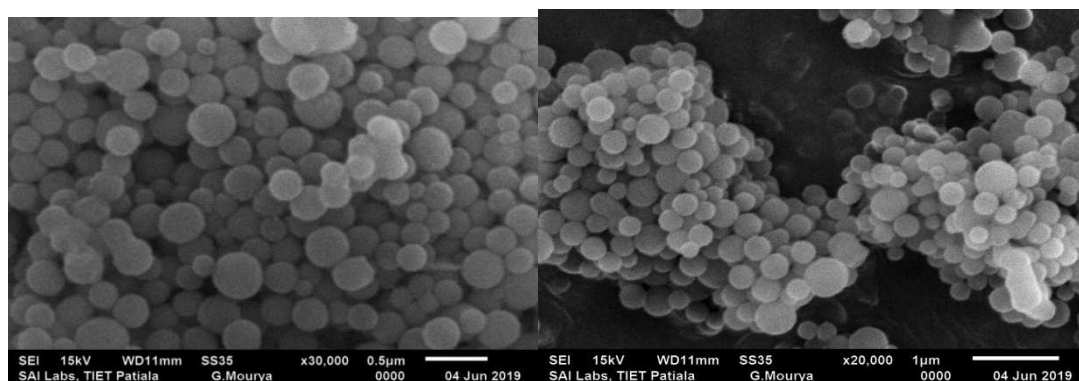
FUNCTIONAL GROUPS	PEAKS (nm)
O-H (broad)	3416
C-H (Stretch)	2928.4
-C=O (Stretch)	1703.6
C-H	1400-1300
C-O	1200-1025
=C-H	800-720

**Figure 4.4:** FTIR spectra showing difference in absorbance in bare- CNS and Fe immobilised CNS. **Table 4.2:** FTIR values of CNS.

**SEM and EDS Analysis:** **Figure 4.5** shows SEM image of spherical CNS synthesized having approximate size of 470nm by hydrothermal method [37]. There was no change in the morphology of CNS after immobilization of iron on to their surface. **Figure 4.5(a) and 4.5(b)** shows SEM images of Fe2CNS and Fe10CNS having same spherical morphology as native CNS **Figure 3.1 (a)**. EDX data shows the composition of the sample.

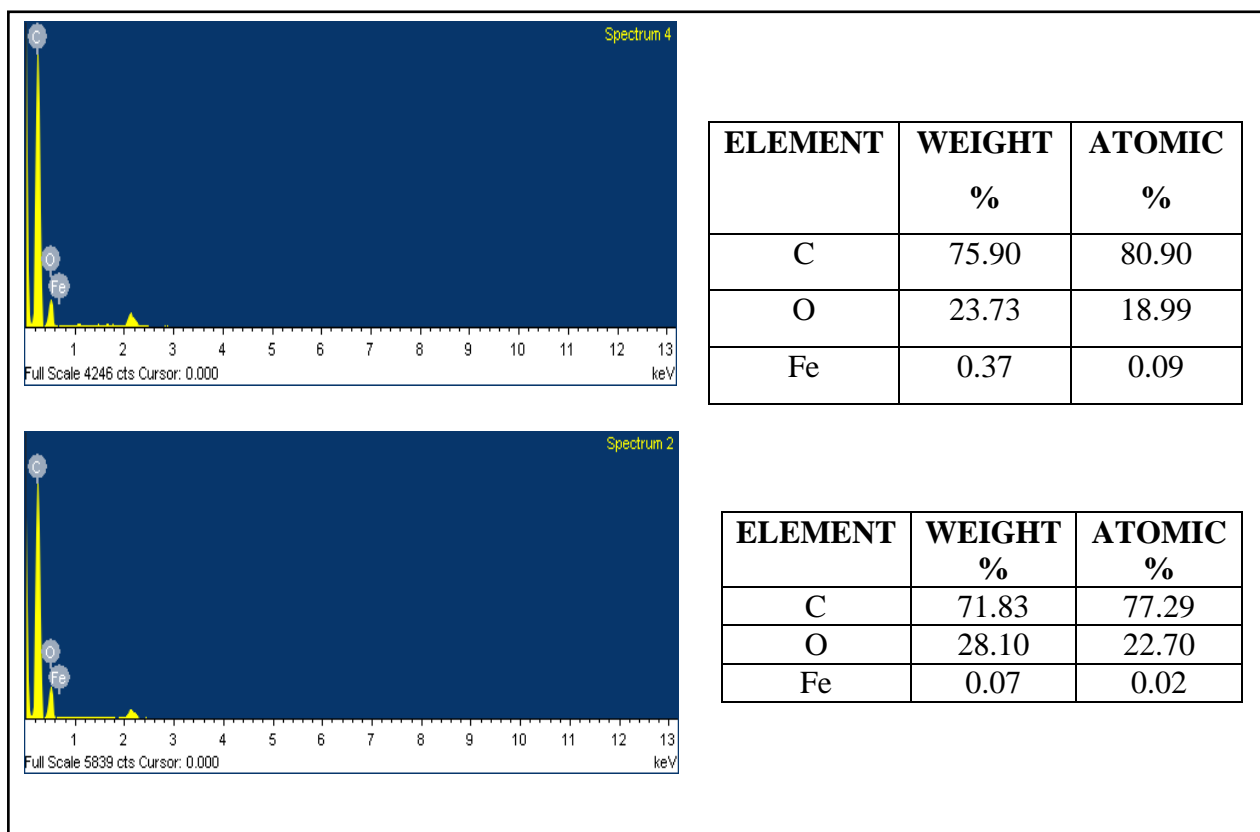


**Figure 4.5: a)** SEM image of Fe2CNS.



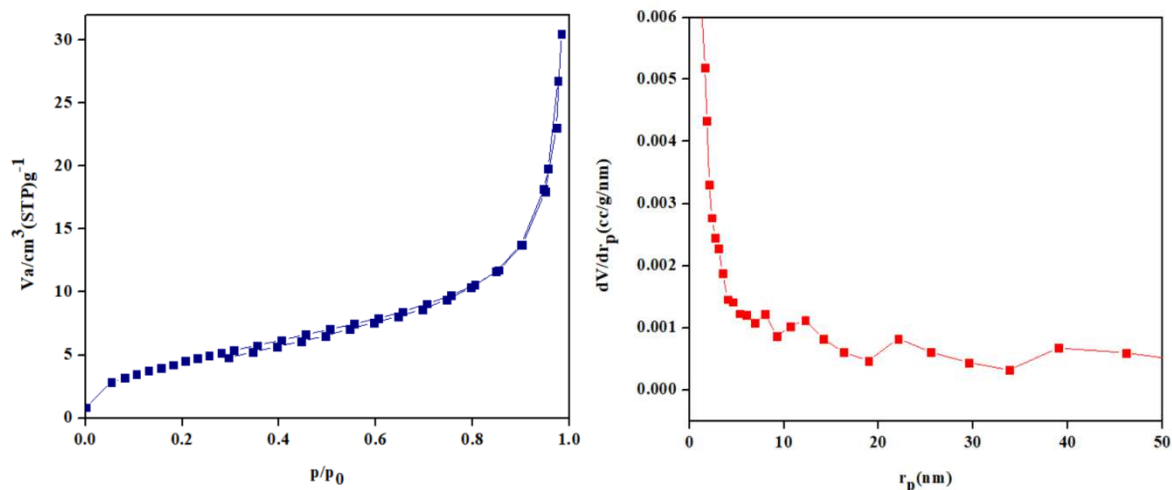
**Figure 4.5: b)** SEM image of Fe10CNS.

Figure 4.6 (a) & (b) shows the percentage of iron (Fe) in both Fe2CNS and Fe10CNS samples as 0.37 and 0.07% respectively. This is in concordance with the conclusions drawn from IR data that is Fe2CNS samples have high iron percentage than Fe10CNS samples due to increased ratio of CNS : Fe-1,10-phenanthraline complex in case of former (2:1) as compared to later (10:1) during their preparation by sonication.



**Figure 4.6:** EDS Data a)Fe2CNS b) P-Fe10CNS and **Table 4.3:** Elements present in sample.

**BET analysis:**Figure 4.7 (a) & (b) shows N<sub>2</sub> adsorption – desorption isotherm and the pore size distribution for the Fe<sub>2</sub>CNS sample. The analysis done using BJH method showses increased surface area ~17.5 m<sup>2</sup>/g and a decrease in mean pore diameter ~10.77nm and total pore volume ~0.0047cm<sup>3</sup>/g as compared to bare-CNS<sup>37</sup>. These results clearly support our earlier conjecture of immobilization of Fe ions on CNS surface.



**Figure 4.7:** a) N<sub>2</sub> adsorption and desorption isotherms of as prepared Fe<sub>2</sub>CNS b) pore size distribution of prepared Fe<sub>2</sub>CNS.

### 4.3APPLICATIONS

**Decolorization activity of CNS for MB dye:** CNSs can be used for decolorization of the MB dye solution either by adsorption in dark or by degradation in the presence of UV light. The bare CNSs result in decolorization of 29.1% in dark and 80% in the presence of UV light.

The decolorization of MB dye solution in the dark shows enhancement for the Fe adsorbed samples: 35% for Fe<sub>2</sub>CNS and 37.5% for Fe<sub>10</sub>CNS. So the adsorption of Fe is enhancing the MB dye adsorption on to the surface of the CNSs. But for too large a coverage as in Fe<sub>2</sub>CNS it falls off. This indicates that there is an optimal coverage by Fe for which the MB dye adsorption will be maximum beyond which it starts to decrease.

Under the UV light, addition of Fe<sub>2</sub>CNS and Fe<sub>10</sub>CNS results in 62%, 64.5% decolorization of MB dye solution. CNSs act as a catalyst for degradation of methylene Blue dye by creating electron hole pairs which lead to oxidation of the dye. The decrease in decolorization efficiency of may be due the presence of Fe on the surface hindering the electron hole pair generation/mobility.

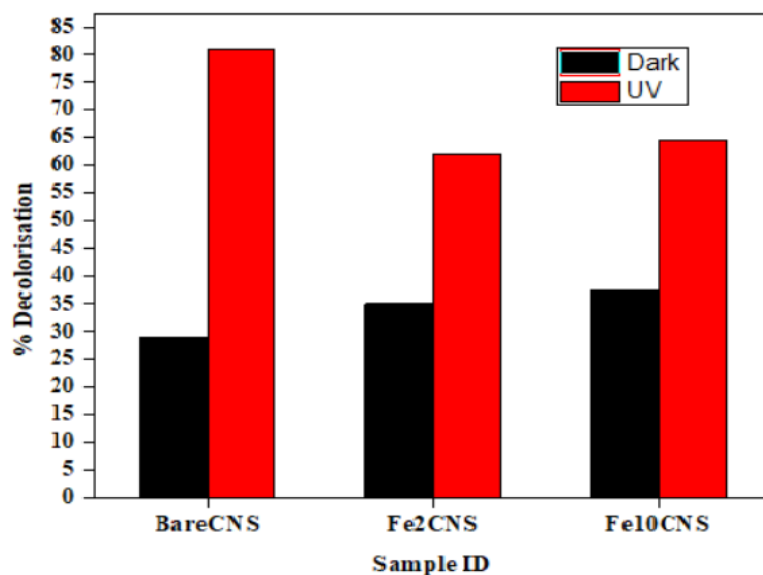
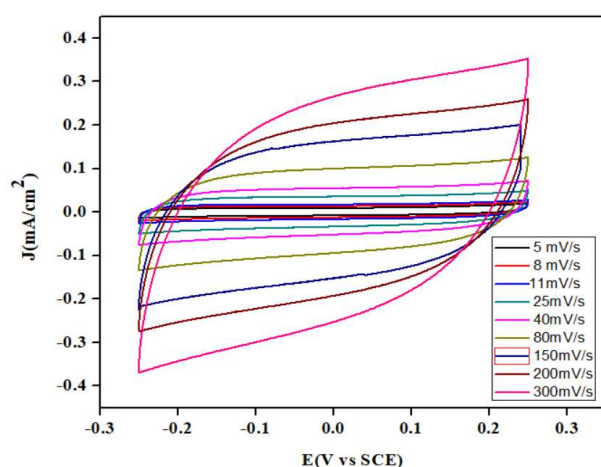


**Figure 4.8:** Showing decolorization of Methylene Blue in dark and under UV light.

**Electrochemical study:** The bare-CNS, Fe2CNS and Fe10CNS are used as working electrode in 3-cell configuration to determine their Electrochemical double layer capacitance ( $C_{dl}$ ). **Figure 4.9** shows cyclic voltammetry results for Fe10CNS obtained for different rates (5 mV/s – 300 mV/s). This is representative for all the samples.

**Figure 4.10 (a)** gives the comparison of CV(at dE/dtof 11 mV/) for the 3 samples bare-CNS, Fe2CNS and Fe10CNS. The data clearly shows that the current densities are enhanced in case of Fe10CNS sample. **Figure 4.10 (b)** clearly shows that Fe10CNS has much higher  $C_{dl}$  as compared to bare CNS (**Table 4.4**).



<b>Table 4.4:</b> Calculated $C_{dl}$ value for samples.	
<b>SAMPLE</b>	<b><math>C_{dl}</math> (mF/cm<sup>2</sup>)</b>
Bare-CNS	0.337
Fe 2CNS	0.278
Fe10CNS	8.75

**Figure 4.9:** Graph plotted between potential and current density showing CV when Fe10CNS is used as working electrode.

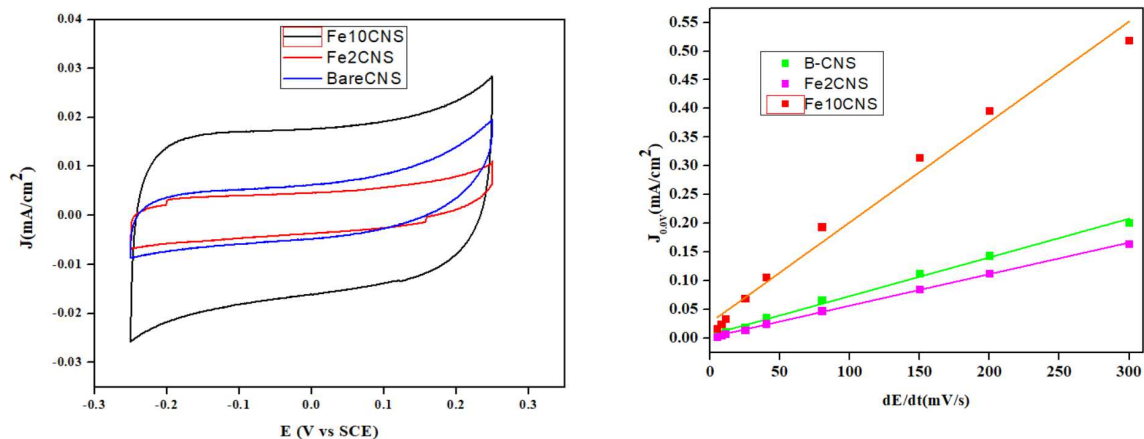


**Figure 4.10:** a) Graph plotted between potential and current density showing comparison of voltammetry cycle between Bare-CNS, Fe2 CNS and Fe10CNS. b)  $C_{dl}$  fits for all the samples.

An interesting result to emerge from these experiments is that initially the presence of Fe enhances the  $C_{dl}$  but for a very large amount of Fe the  $C_{dl}$  values actually decreases and even become lower than the bare samples (for Fe2CNS). This indicates that there is an optimum value of Fe coverage for enhancing the  $C_{dl}$  value beyond which the Fe actually deteriorates the capacitance of the samples.

## CHAPTER 5

---

### CONCLUSION

Red coloured tris-(1,10-phenanthroline) iron(II) complex was prepared by dissolving  $\text{FeSO}_4$  and 1,10 phenanthroline in ethanol. The complex was further used to immobilize iron on carbon nanospheres by sonicating the solution for 1 hour at room temperature, which led to formation of Fe2CNS, Fe5CNS and Fe10CNS. BET surface area analysis displayed increased surface area and pore size as compared to bare CNS. The material was then used for decolouration of methylene blue dye (MB) solution both by adsorption in dark and by degradation in the presence of UV light. The decolorization of MB dye solution in the dark shows enhancement for the Fe adsorbed samples: 35% for Fe2CNS and 37.5% for Fe10CNS but for large coverage of iron it falls. Under the UV light, addition of Fe2CNS and Fe10CNS results in 62%, 64.5% decolorization of MB dye solution. The degradation of dye was less in case of iron immobilized CNS as fewer amounts of electron pair are generated. Prepared samples were used in electrochemical studies as working electrode for supercapacitor.  $C_{dl}$  fits for all the samples were plotted and highest value was in case of Fe10CNS as Fe was providing extra charge which will lead to increase in potential and CV.

### SCOPE IN FUTURE

The immobilization of Fe is needed to be done on CNS by varying the concentration of tris (1,10phenanthroline ) iron(ii) sulphate complex, and to determine the optimum coverage the  $C_{dl}$  value is highest. New metal complexes are needed to be synthesised which can be further used for immobilization on CNS. There is a need to know which metal immobilized on CNS results in the highest enhancement of  $C_{dl}$ . Charging and discharging curve of sample have to be performed and to check the value of capacitance of pseudo capacitor and Electrochemical double layer capacitator individually.

## REFERENCES

---

1. Nasir, S.; Hussein, M. Z.; Zainal, Z.; Yusof, N. A., Carbon-Based Nanomaterials/Allotropes: A Glimpse of Their Synthesis, Properties and Some Applications, *Materials*, **2018**, 11, 295, 1-24.
2. Shah, R.; Kausar, A.; Muhammad, B.; Shah, S., Progression from Graphene and Graphene Oxide to High Performance Polymer-Based Nanocomposite: A Review, *Polymer-Plastics Technology and Engineering*, **2015**, 54, 173–183.
3. Bakey, R.; Vallant, R. M.; Najam-ul-Haq, M.; Rainer, M.; Szabo, Z.; Huck, C. W.; Bonn, G.K.; Medicinal applications of fullerenes. *Int J Nanomedicine* **2007**, 2, 639-49.
4. Iijima, S., Helical microtubules of graphitic carbon, *Nature*, **1991**, 354, 56–58.
5. Nieto-Marquez, A.; Romero, R.; Romero, A.; Valverde, J. L., Carbon nanospheres: synthesis, physicochemical properties and applications. *J. Mater. Chem.*, **2011**, 21, 1664–72.
6. Coville, N. J.; Mhlanga, S. D.; Nxumalo, E. N.; Skaikjee, A., A review of shaped carbon nanomaterials. *South African Journal of Science* **2011**, 107, 01-15.
7. Wang, Y.; Li, Z.; Wang, J.; Li, J.; Lin, Y., Graphene and graphene oxide: biofunctionalization and applications in biotechnology. *Trends in Biotechnology* 2011, 29, 205-12.
8. Allen, M. J.; Tung, V. C.; Kaner, R. B., Honeycomb Carbon: A Review of Graphene. *Chem Rev* **2010**, 110, 132-45.
9. Shah, R.; Kausar, A.; Muhammad, B.; Shah, S., Progression from Graphene and *Taylor & Francis Group* **2015**, 54, 173-83.
10. Jo, G.; Choe, M.; Lee, S.; Park, W.; Kahng, Y. H.; Lee, T., The Application of graphene as electrodes in electrical and optical devices, *Nanotechnology*, **2012**, 23, 2-19.
11. Choi, W.; Lahiri, I.; Seelaboyina, R.; Kang, Y. S., Synthesis of graphene and Its Applications: Review. *Critical Review in Solid State and Material Sciences* **2010**, 35, 52-71.
12. Zhang, P.; Qiao, Z.-A.; Dai, S., Recent advances in carbon nanospheres: synthetic routes and applications. *Chem. Commun.*, **2015**, 51, 9246-56.
13. Qu, L.; Zhang, H.; Zhu, J.; Dai, L., Tunable assembly of carbon nanospheres on single-walled carbon nanotubes. *Nanotechnology* **2010**, 21, 2-8.

14. Karna, P.; Ghimire, M.; Mishra, S.; Karna, S., Synthesis and Characterization of Carbon Nanospheres. *OALib Journal***2017**, 4, 1-7.
15. Pathak, S.; Greci, M. T.; Kwong, R. C.; Mercado, K.; Prakash, G. K. S.; Olah, G. A.; Thompson, M. E., Synthesis and Applications of Palladium-Coated Poly(vinylpyridine) Nanospheres. *Chem. Mater.*,**2000**, 12, 1985-89.
16. Liang, H-P.; Zhang, H-M.; Hu, J-S.; Guo, Y.; Wan, L-J.; Bai, C-L., Pt Hollow Nanospheres: Facile Synthesis and Enhanced Electrocatalysts. *Angew. Chem. Int. Ed.* **2004**, 43, 1540–43.
17. Shukla, S.; Priscilla, A.; Banerjee, M.; Bhonde, R. R.; Ghatak, J.; Satyam, P. V.; Sastry, M., Porous Gold Nanospheres by Controlled Transmetalation Reaction: A Novel Material for Application in Cell Imaging. *Chem. Mater.***2005**, 17, 5000-05.
18. Zhang, J.; Liu, J.; Peng, Q.; Wang, X.; Li, Y., Nearly Monodisperse Cu<sub>2</sub>O and CuO Nanospheres: Preparation and Applications for Sensitive Gas Sensors. *Chem. Mater.***2006**, 18, 867-71.
19. Frackowiak, E., Carbon materials for supercapacitor application. *Phys. Chem. Chem. Phys.*,**2007**, 9, 1774–85.
20. Qiao, W. M.; Song, Y.; Lim, S. Y.; Hong, S. H.; Yoon, S. H.; Mochida, I.; Imaoka, T., Carbon nanospheres produced in an arc-discharge process. *Carbon***2006**, 44, 158–193.
21. Bhagat, P. N.; Patil, K. R.; Bodasa, D. S.; Paknikar, K. M., Hydrothermal synthesis and characterization of carbon nanospheres: a mechanistic insight. *J. Name.*, **2013**, 1-3.
22. Zou, G.; Yu, D.; Lu, J.; Wang, D.; Jiang, C.; Qian, Y., A self-generated template route to hollow carbon nanospheres in a short time. *Solid State Communications***2004**, 131, 749–752.
23. Shang, S.; Zeng, W.; Tao, X-M., Highly Stretchable Conductive Polymer Compositing with Carbon Nanotubes and Nanospheres. *Advanced Materials Research*, **2010**, 109-112.
24. Tang, K.; Fu, L.; White, R. J.; Yu, L.; Titirici, M. M.; Antonietti, M.; Maier, J., Hollow Carbon Nanospheres with Superior Rate Capability for Sodium-Based Batteries. *Adv. Energy Mater.***2012**, 2, 873–877.
25. Thomas, P.; Billaud, D., Electrochemical insertion of sodium into hard carbons. *Electrochimica Acta***2002**, 47, 3303-07.
26. Li, M.; Wang, C.; Connell, M. J.; Chan, C. K., Carbon nanosphere adsorbents for removal of arsenate and selenate from water. *Environ. Sci.: Nano*, **2015**, 2, 245–250.

27. Vié, R.; Drahi, E.; Baudino, O.; Blayac, S.; Berthon-Fabry, S., Synthesis of carbon nanospheres for the development of inkjetprinted resistive layers and sensors. *Flex. Print. Electron*, **2016**, 1-10.
28. Qiao, X.; Peng, H.; You, C.; Liu, F.; Zheng, R.; Xu, D.; Li, X.; Liao, S., Nitrogen, phosphorus and iron doped carbon nanospheres with high surface area and hierarchical porous structure for oxygen reduction. *Journal of Power Sources* **2015**, 288, 253 -260.
29. Wang, H.; Li, X.; Ma, Z.; Wang, D.; Wang, L.; Zhan, J.; She, L.; Yang, F., Hydrophilic mesoporous carbon nanospheres with high drug-loading efficiency for doxorubicin delivery and cancer therapy. *International Journal of Nanomedicine*, **2016**, 11, 1793-1806.
30. Zhang, W.; Wang, F.; Li, X.; Liua, Y.; Liua, Y.; Maa, J., Fabrication of hollow carbon nanospheres introduced with Fe and N species immobilized palladium nanoparticles as catalysts for the semihydrogenation of phenylacetylene under mild reaction conditions. *Applied Surface Science*, **2017**, 404, 398–408.
31. Gupta, D.; Saha, B., Carbon nanosphere supported Ru catalyst for the synthesis of renewable herbicide and chemicals. *Catalysis Communications*, **2017**, 100, 206–09.
32. Zhao, Z.; Ma, X.; Wang, X.; Ma, Y.; Liu, C.; Hang, H.; Zhang, Y.; Du, Y.; Ye, W., Synthesis of amorphous PdP nanoparticles supported on carbon nanospheres for 4-nitrophenol reduction in environmental applications. *Applied Surface Science*, **2018**, 1-24.
33. Taoa, X.; Zhangb, Q.; Lia, Y.; Lv, X.; Mac, D.; Wanga, H-G., N, P, S tri-doped hollow carbon nanosphere as a high-efficient bifunctional oxygen electrocatalyst for rechargeable Zn-air batteries. *Applied Surface Science* **2019**, 490, 47–55.
34. Wang, J.; Fan, M.; Tu, W.; Chen, K.; Shen, Y.; Zhang, H., In situ growth of Co<sub>3</sub>O<sub>4</sub> on nitrogen-doped hollow carbon nanospheres as air electrode for lithium-air batteries. *Journal of Alloys and Compounds* **2019**, 777, 944-53.
35. Wang, G.; Qin, J.; Zhao, Y.; Wei, J., Nanoporous carbon spheres derived from metal-phenolic coordination polymers for supercapacitor and biosensor. *Journal of Colloid and Interface Science*, **2019**, 544, 241–248.
36. Song, X.; Gunawan, P.; Jiang, R.; Leong, S. S.J.; Wang, K.; Xu, R., Surface activated carbon nanospheres for fast adsorption of silver ions from aqueous solutions. *Journal of Hazardous Materials* **2011**, 194, 162–68.

37. Bhatnagar, D.; Kumar, A.; Chaudhary, R.; Brar, K. L.; Chhibber, M., A Convenient Method to Aggregate CNS by Tagging with Diphenyl Ether Molecule. *AIP Conference proceedings*, **2019**, 2115, 1-4.
38. Kumar, A.; Kumar, P.; Paul, S.; Jain, S. L., Visible Light assisted reduction of nitrobenzenes using  $\text{Fe}(\text{bpy})_3^{+2}/\text{rGO}$  nanocomposite as photocatalyst. *Applied Surface Science*, **2016**, 386, 103-114.

# Thesis

## ORIGINALITY REPORT

12%

SIMILARITY INDEX

4%

INTERNET SOURCES

6%

PUBLICATIONS

7%

STUDENT PAPERS

## PRIMARY SOURCES

1	Submitted to Thapar University, Patiala Student Paper	3%
2	Submitted to United States Air Force Academy Student Paper	1%
3	onlinelibrary.wiley.com Internet Source	1%
4	buyersguide.homesandland.com Internet Source	1%
5	Li, Man, Chengwei Wang, Michael J. O'Connell, and Candace K. Chan. "Carbon nanosphere adsorbents for removal of arsenate and selenate from water", Environmental Science Nano, 2015. Publication	1%
6	ira.lib.polyu.edu.hk Internet Source	1%
7	www.dovepress.com Internet Source	<1%

Xisheng Tao, Qi Zhang, Yan Li, Xiaoling Lv,

*Xisheng Tao*

**8** Delong Ma, Heng-guo Wang. "N, P, S tri-doped hollow carbon nanosphere as a high-efficient bifunctional oxygen electrocatalyst for rechargeable Zn-air batteries", Applied Surface Science, 2019  
Publication <1%

---

**9** Rémy Vié, Etienne Drahi, Olivier Baudino, Sylvain Blayac, Sandrine Berthon-Fabry. "Synthesis of carbon nanospheres for the development of inkjet-printed resistive layers and sensors", Flexible and Printed Electronics, 2016  
Publication <1%

---

**10** Dinesh Gupta, Basudeb Saha. "Carbon nanosphere supported Ru catalyst for the synthesis of renewable herbicide and chemicals", Catalysis Communications, 2017  
Publication <1%

---

**11** epdf.tips  
Internet Source <1%

---

**12** Horacio A. Mottola. "Some considerations on reaction rate methods—the analytical use of modifying effects of ligands in some electron-transfer reactions", Analytica Chimica Acta, 1974  
Publication <1%

---

**13** Junbo Wang, Meiling Fan, Wenmao Tu, Kai

---

Chen, Yafei Shen, Haining Zhang. "In situ growth of Co<sub>3</sub>O<sub>4</sub> on nitrogen-doped hollow carbon nanospheres as air electrode for lithium-air batteries", Journal of Alloys and Compounds, 2019

Publication

<1%

---

14

Submitted to University of Sheffield

Student Paper

<1%

---

15

Submitted to Higher Education Commission Pakistan

Student Paper

<1%

---

16

Li, Sen, and Seiichi Ishikawa. "Hydroxyl radical rinse water technology using ozone ultrasonic ultraviolet and TiO<sub>2</sub>", 2011 International Symposium on Water Resource and Environmental Protection, 2011.

Publication

<1%

---

17

Submitted to Middle East Technical University

Student Paper

<1%

---

18

Su, Dawei, Katja Kretschmer, and Guoxiu Wang. "Improved Electrochemical Performance of Na-Ion Batteries in Ether-Based Electrolytes: A Case Study of ZnS Nanospheres", Advanced Energy Materials, 2015.

Publication

<1%

---

19

pubs.acs.org

Internet Source

<1%

20	Submitted to Universiti Malaysia Kelantan Student Paper	<1%
21	Submitted to Nottingham Trent University Student Paper	<1%
22	Hou, Hongshuai, Mingjun Jing, Yingchang Yang, Yirong Zhu, Laibing Fang, Weixin Song, Chengchi Pan, Xuming Yang, and Xiaobo Ji. "Sodium/Lithium Storage Behavior of Antimony Hollow Nanospheres for Rechargeable Batteries", ACS Applied Materials & Interfaces Publication	<1%
23	www.sciencedomain.org Internet Source	<1%
24	Chengxing Li, Daobin Liu, Yukun Xiao, Zixuan Liu, Li Song, Zhipan Zhang. " Mesoporous Co O -Rods-Entangled Carbonized Polyaniline Nanotubes as an Efficient Cathode Material toward Stable Lithium–Air Batteries ", ACS Applied Energy Materials, 2019 Publication	<1%
25	Mary M. Walczak, Nolan T. Flynn. "Spectroelectrochemical study of the generation of tris-(1,10-phenanthroline) iron(II/III) from $\mu$ -oxo-bis[aquabis(1,10-phenanthroline) iron(III)]", Journal of Electroanalytical Chemistry, 1998 Publication	<1%

26

Submitted to Queen Mary and Westfield College  
Student Paper

<1%

Exclude quotes  On

Exclude matches  < 8 words

Exclude bibliography  On